Noninvasively determined muscle oxygen saturation is an early indicator of central hypovolemia in humans

Babs R. Soller,[1] Ye Yang,[1] Olusola O. Soyemi,[1] Kathy L. Ryan,[2] Caroline A. Rickards,[2] J. Matthias Walz,[1] Stephen O. Heard,[1] and Victor A. Convertino[2]

[1]*Department of Anesthesiology, University of Massachusetts Medical School, Worcester, Massachusetts; and* [2]*U. S. Army Institute of Surgical Research, Fort Sam Houston, Texas*

Submitted 5 June 2007; accepted in final form 13 November 2007

Soller BR, Yang Y, Soyemi OO, Ryan KL, Rickards CA, Walz JM, Heard SO, Convertino VA. Noninvasively determined muscle oxygen saturation is an early indicator of central hypovolemia in humans. *J Appl Physiol* 104: 475–481, 2008. First published November 15, 2007; doi:10.1152/japplphysiol.00600.2007.—Ten healthy human volunteers were subjected to progressive lower body negative pressure (LBNP) to the onset of cardiovascular collapse to compare the response of noninvasively determined skin and fat corrected deep muscle oxygen saturation (SmO_2) and pH to standard hemodynamic parameters for early detection of imminent hemodynamic instability. Muscle SmO_2 and pH were determined with a novel near infrared spectroscopic (NIRS) technique. Heart rate (HR) was measured continuously via ECG, and arterial blood pressure (BP) and stroke volume (SV) were obtained noninvasively via Finometer and impedance cardiography on a beat-to-beat basis. SmO_2 and SV were significantly decreased during the first LBNP level (-15 mmHg), whereas HR and BP were late indicators of impending cardiovascular collapse. SmO_2 declined in parallel with SV and inversely with total peripheral resistance, suggesting, in this model, that SmO_2 is an early indicator of a reduction in oxygen delivery through vasoconstriction. Muscle pH decreased later, suggesting an imbalance between delivery and demand. Spectroscopic determination of SmO_2 is noninvasive and continuous, providing an early indication of impending cardiovascular collapse resulting from progressive reduction in central blood volume.

tissue oxygen; near infrared spectroscopy; physiological monitoring; hemodynamic instability; lower body negative pressure

TRAUMA AND SEVERE HEMORRHAGE remain the most frequent causes of death in the 1–44 yr age group in both the civilian and military settings (2, 4, 24). Early recognition of the severity of shock and prompt institution of appropriate resuscitative measures are widely believed to improve outcome and decrease the progression to multi-system organ failure by virtue of maintaining end-organ perfusion. Routine clinical parameters such as arterial blood pressure, heart rate (HR), mental status, and urine output, as well as hematocrit levels, are often late indicators of the true extent of metabolic derangement during hypovolemic shock. In a study on HR variability and its association with mortality in prehospital trauma patients, Cooke and Convertino (8) demonstrated that HR, arterial oxygen saturation (via pulse oximetry), and arterial blood pressure were poor predictors of outcome. Hence, there exists a need for noninvasive, continuous monitoring of parameters that can provide an early indication of central hypovolemia.

The physiological response to hemorrhage includes significant vasoconstriction to help maintain adequate perfusion pressure to vital organs. In swine models of hemorrhage, this can be observed as an early, rapid, and significant decrease in peripheral and splanchnic oxygenation (3, 26) as blood is shunted to the heart and brain. On the basis of this known physiological response, we hypothesize that a noninvasive assessment of muscle oxygen could provide a significantly earlier indication of blood volume loss than the standard vital sign measurements.

Near infrared spectroscopy (NIRS) is in wide clinical use for the determination of arterial oxygen saturation (Sa_{O_2}), which provides information on pulmonary gas exchange. When blood flow to the peripheral muscles is decreased, an increase in oxygen extraction is reflected in a reduction in muscle oxygen saturation (SmO_2; Ref. 3) and muscle oxygen tension (PmO_2; Ref. 28), both of which can be determined noninvasively with NIRS. It is also possible to determine muscle pH (pHm) using NIRS (28, 37). In swine hemorrhage, tissue pH is significantly more sensitive to shock than measures of arterial and venous pH (26), and depressed tissue pH is strongly associated with negative outcomes (27). From a practical standpoint, NIRS instruments can be made small and portable, allowing them to be used for rapid, noninvasive patient assessment both inside and outside the hospital.

Human models for the controlled study of acute hemorrhage and hemorrhagic shock are very limited because of ethical issues associated with the withdrawal of large volumes of blood from healthy human subjects (18). However, a noninvasive human model for assessing acute, progressive central hypovolemia such as that seen in hemorrhagic shock is based on the use of lower body negative pressure (LBNP). Human volunteers can be subjected to increasing levels of negative pressure applied to the lower body, thus creating central hypovolemia that induces hemodynamic responses similar to those reported during acute hemorrhage (9). We thus used the LBNP model to assess the response of noninvasively determined SmO_2 and pHm to central hypovolemia. On the basis of previous animal studies, we hypothesized that SmO_2 and PmO_2 would provide a very early indicator of central hypovolemia, while significant changes in pHm would only occur later in the hypovolemic challenge when an imbalance between oxygen delivery and demand developed.

MATERIALS AND METHODS

Subjects. Ten healthy, non-smoking, normotensive men and women (5/5) with a mean ($\pm$SE) age of 35 $\pm$ 3 yr, height 173 $\pm$ 5 cm,

			Form Approved	
			OMB No. 0704-0188	

Report Documentation Page

1. REPORT DATE	2. REPORT TYPE	3. DATES COVERED
01 FEB 2008	**N/A**	**-**

4. TITLE AND SUBTITLE	5a. CONTRACT NUMBER
Noninvasively determined muscle oxygen saturation is an early indicator of central hypovolemia in humans	5b. GRANT NUMBER
	5c. PROGRAM ELEMENT NUMBER
6. AUTHOR(S)	5d. PROJECT NUMBER
Soller B. R., Yang Y., Soyemi O. O., Ryan K. L., Rickards C. A., Walz J. M., Heard S. O., Convertino V. A.,	5e. TASK NUMBER
	5f. WORK UNIT NUMBER

7. PERFORMING ORGANIZATION NAME(S) AND ADDRESS(ES)	8. PERFORMING ORGANIZATION REPORT NUMBER
United States Army Institute of Surgical Research, JBSA Fort Sam Houston, TX 78234	

9. SPONSORING/MONITORING AGENCY NAME(S) AND ADDRESS(ES)	10. SPONSOR/MONITOR'S ACRONYM(S)
	11. SPONSOR/MONITOR'S REPORT NUMBER(S)

12. DISTRIBUTION/AVAILABILITY STATEMENT
Approved for public release, distribution unlimited

13. SUPPLEMENTARY NOTES

14. ABSTRACT

15. SUBJECT TERMS

16. SECURITY CLASSIFICATION OF:			17. LIMITATION OF ABSTRACT	18. NUMBER OF PAGES	19a. NAME OF RESPONSIBLE PERSON
a. REPORT	b. ABSTRACT	c. THIS PAGE	**UU**	**7**	
unclassified	**unclassified**	**unclassified**			

Standard Form 298 (Rev. 8-98)
Prescribed by ANSI Std Z39-18

and weight 75 ± 6 kg volunteered to participate as subjects for this investigation. All procedures and risks associated with the study were explained and voluntary written informed consent was obtained from the participants. A complete medical history and physical examination was performed on each of the potential subjects. In addition, female subjects underwent a urine test to ensure that they were not pregnant. Subjects maintained their normal sleep pattern, refrained from exercise, and abstained from caffeine and other autonomic stimulants such as prescription or non-prescription drugs for at least 48 hr prior to the experimental protocol unless cleared by the physician medical screener to continue taking the medications. All experimental procedures and protocols were reviewed and approved by the Institutional Review Board for the use of human subjects at the Brooke Army Medical Center at Fort Sam Houston, TX.

Protocol. With the use of a neoprene skirt designed to form an airtight seal between the subject and the chamber, the application of negative pressure to the lower body (below the iliac crest) results in a redistribution of blood away from the upper body (head and heart) to the lower extremities and abdomen. This model provides conditions of controlled, experimentally induced hypovolemic hypotension, offering a valuable method for investigating monitoring devices such as NIRS. Although absolute equivalence between the magnitudes of negative pressure applied and actual blood loss cannot be determined at this time, review of human and animal data has revealed ranges of effective blood loss (or fluid displacement) caused by LBNP. On the basis of the magnitude of induced central hypovolemia, we estimate that 10–20 mmHg negative pressure produces hemodynamic responses equivalent to those resulting from blood loss of 400–550 ml; 20–40 mmHg LBNP induces hemodynamic responses equivalent to blood loss of 550–1,000 ml; while >40 mmHg LBNP induces responses equivalent to blood loss approximating 1,000 ml or more (9).

Each subject reported to the laboratory for a progressive LBNP protocol that was designed to test his/her tolerance to experimentally induced hypotensive hypovolemia. The subject was first instrumented with noninvasive devices to measure HR, stroke volume (SV), arterial blood pressure, PmO₂, and pHm. The LBNP protocol consisted of a 5-min baseline period followed by 5 min of chamber decompression to −15, −30, −45, and −60 mmHg and additional increments of −10 mmHg every 5 min until either the onset of cardiovascular collapse or the completion of 5 min at −100 mmHg. Cardiovascular collapse was defined by one or a combination of the following criteria: *1*) a precipitous fall in systolic blood pressure (SBP) >15 mmHg and/or sudden bradycardia; *2*) progressive diminution of SBP <70 mmHg; or *3*) voluntary subject termination due to discomfort from presyncopal symptoms such as sweating, nausea, dizziness, or gray-out. At the onset of cardiovascular collapse, the chamber vacuum was released to ambient pressure to rapidly restore blood flow to the central compartment. To assure subject safety, an ACLS-certified physician was present in the laboratory building during all LBNP tests.

Hemodynamic measurements. Continuous HR was measured from a standard electrocardiogram (ECG). Beat-by-beat SBP and diastolic blood pressure (DBP) were measured noninvasively using an infrared finger photoplethysmograph (Finometer Blood Pressure Monitor, TNO-TPD Biomedical Instrumentation, Amsterdam, The Netherlands). The Finometer blood pressure cuff was placed on the middle finger of the left hand, which, in turn, was laid at heart level. Excellent estimates of directly measured intra-arterial pressures during various physiological maneuvers have been demonstrated with this device (15, 16, 21, 33). Mean arterial pressure (MAP) was calculated by dividing the sum of SBP and twice DBP by three. Pulse pressure (PP) was calculated by subtracting DBP from SBP. Arterial oxygen saturation was measured using pulse oximetry (BCI Capnocheck Plus; Smiths Medical, Waukesha, WI).

While the Finometer is capable of determining SV and total peripheral resistance (TPR), superior accuracy in this setting has been observed with the thoracic bioimpedance technique (20). Beat-to-beat SV was measured noninvasively using thoracic electrical bioim-

pedance with an HIC-2000 Bio-Electric Impedance Cardiograph (Bio-Impedance Technology, Chapel Hill, NC). This technique is based on the resistance changes in the thorax to a low-intensity (4 mA), high-frequency (70 kHz) alternating current applied by band electrodes placed at the root of the neck at the xiphoid process at the midaxillary line. Ventricular SV was determined via the Kubicek equation (17): SV (in ml) = $\rho \times (L/Z_0)^2 \times$ LVET $\times$ (dZ/dt), where ρ (in ohm/cm) is the blood resistivity, a constant of 135 ohms/cm in vivo; L (in cm) is the mean distance between the inner band electrodes (front and back); Z_0 (in ohms) is the average thoracic background impedance; LVET (in seconds) is the left ventricular ejection time; and (dZ/dt) is the maximum height of the dZ/dt peak measured from the zero line. Correlation coefficients of 0.70–0.93 have been reported in SV measurements simultaneously made with thoracic electrical bioimpedance and thermodilution techniques (20). Cardiac output (Q) was calculated as the product of HR and SV, and TPR was estimated by dividing MAP by Q.

Hemodynamic data were sampled at 500 Hz and recorded directly to data-acquisition software (WINDAQ, Dataq Instruments, Akron, OH). Analysis of data was subsequently accomplished using commercially available analysis software (WinCPRS, Absolute Aliens, Turku, Finland). Data presented for each of these parameters represent the average values taken over the last 3 min of baseline and each LBNP level.

Noninvasive determination of SmO₂, PmO₂, and pHm. SmO₂, PmO₂, and pHm were determined noninvasively using a NIRS monitor developed jointly by personnel from the Anesthesiology Department of the University of Massachusetts Medical School (Worcester, MA) and Luxtec (West Boylston, MA). This spectroscopic technique was validated for individual heart surgery patients against invasive PO₂ and pH sensors inserted into the hypothenar muscle (28). The NIRS system used in this study employs additional mathematical preprocessing techniques to correct spectra for variation in skin pigmentation, fat, and muscle optical properties prior to the calculation of SmO₂, PmO₂, and pHm. These techniques are necessary to allow one calibration equation for each parameter to be used for all subjects. The optical sensor collects NIR reflectance spectra from deep within the forearm muscle (flexor digitorum profundus) every ~20 s. The spectra are then processed with calibration equations contained in a dedicated computer. SmO₂, PmO₂, and pHm are simultaneously calculated from each spectrum, displayed as a trend, and stored on a hard drive contained in the system.

Light is collected with two sensors contained in the same housing. One sensor collects light that illuminates only the skin and fat layer. The second sensor collects light that illuminates the skin, fat, and muscle layer. Mathematical processing removes the light reflected from the skin and fat, leaving only the absorption spectrum of muscle (34). Removal of spectral interference from skin pigmentation and fat is critical to determining absolute chemical concentrations from muscle spectra. The mathematical equations for determining SmO₂ and PmO₂ from the corrected spectra are briefly described in the APPENDIX. A detailed description of the SmO₂ calculation and its validation has recently been published by Yang et al. (36). PmO₂ is calculated from the SmO₂ determination. Since NIRS cannot distinguish myoglobin absorbance from hemoglobin absorbance, SmO₂ refers to combined saturation of hemoglobin and myoglobin and PmO₂ refers to partial pressure of oxygen in the interstitial fluid. The same absorption spectra are also processed by the computer to calculate pH. Subject-to-subject differences in muscle fiber structure produce optical variations that are corrected prior to pH calculation (35). The corrected spectra are then statistically related to previously determined invasive measurements of interstitial fluid pH to produce the calibration equation (28, 37). This second calibration equation is also contained in the computer and used to calculate pHm from the corrected spectra.

The light output of the system is assessed with three NIST-traceable reflectance standards (Avian Technologies, Wilmington, OH) with nominal values of 2, 50, and 99% prior to use on each

subject to allow for determination of the absolute values of SmO_2, PmO_2, and pHm (29).

Statistical analysis. Values for NIRS measurements and hemodynamic parameters are presented as the mean $\pm$ SE. Data from all the noninvasive sensors were collected continuously. For each LBNP level, the last 3 min of data for each measured parameter were averaged to provide a single value for that level.

To evaluate the overall relationship between SV and TPR and SmO_2, the percentage change from baseline was calculated to compensate for different baseline values between subjects. Each measured parameter was analyzed using a linear mixed model analysis of variance with a first order autoregressive covariance structure to determine if there was a significant variation during progressive LBNP. This type of analysis takes into account the repeated nature of the experimental design. If statistical differences were found, Bonferroni-corrected comparisons with baseline measurements were performed to determine the first level of LBNP that could be distinguished statistically from baseline ($P < 0.05$). Statistical analysis was performed using SPSS (version 14.0, SPSS, Chicago, IL).

RESULTS

All 10 subjects completed the study. Six subjects reached cardiovascular collapse at -80 mmHg LBNP and four at -90 mmHg LBNP. In all subjects, HR returned to baseline within 1 min after the LBNP was terminated. Baseline values for specific hemodynamic and NIRS-determined metabolic parameters, the value at which each parameter was statistically different from baseline, and the level of LBNP at which this change was detected are presented in Table 1. Arterial oxygen saturation was not altered from its average baseline value of 98% throughout the entire LBNP protocol. MAP was only sensitive to the detection of impending cardiovascular collapse in that it essentially signaled the end of the LBNP protocol. HR changed significantly during the -60 mmHg level, while PP decreased significantly during the -45 mmHg level. SV was the most sensitive of the hemodynamic parameters, with a significant decrease occurring at the first level of LBNP (-15 mmHg). Early (-15 mmHg LBNP) metabolic indicators of hemodynamic instability included PmO_2 and SmO_2 determined by NIRS. In contrast, pH did not decrease from baseline until -70 mmHg.

Figure 1 shows the average ($n = 10$) of each of the measured and calculated parameters for every level of LBNP through -80 mmHg. HR and PP were unresponsive until -45 mmHg, when HR began to climb and PP decreased. SV, PmO_2, and SmO_2 responses were more sensitive, decreasing from the onset of LBNP (-15 mmHg) and continuing to decrease with the application of greater negative pressure. Muscle pH was

unaltered until -70 mmHg, when it began to significantly fall. The overall change in the absolute value of pHm was very small (0.03 pH units).

Figure 2 illustrates the mean percentage change from baseline for SmO_2 compared with SV (Fig. 2*A*) and TPR (Fig. 2*B*) for each level of LBNP. As LBNP progressed, SmO_2 declined in parallel with SV ($r^2 = 0.96$) and inversely with TPR ($r^2 = 0.94$). PmO_2 was also highly correlated with SV ($r^2 = 0.94$) and TPR ($r^2 = 0.93$).

DISCUSSION

The major finding of this study is that muscle oxygen (either SmO_2 or PmO_2) determined noninvasively with a novel NIRS methodology was correlated with SV and was the earliest indicator of progressive central hypovolemia in human volunteers. The reductions in SV, SmO_2, and PmO_2 were apparent at an LBNP level that represented an equivalent blood loss of only 400–500 ml (9). Perhaps more importantly, reductions in muscle oxygen were detected much earlier than the standard clinical measures of HR and BP. A further finding from this study is that a small but significant decrease in noninvasively measured pHm was observed near the same time as an increase in HR, but later than a detectable change in PP.

The observation that decreases in SmO_2 proportionately tracked the progressive fall in SV throughout the course of the LBNP protocol suggests that this noninvasive measurement is a sensitive marker of a limited Q and delivery of blood to peripheral tissues during central hypovolemia. Likewise, the inverse linear relationship between SmO_2 and TPR implies that skeletal muscle vasoconstriction and a subsequent reduction in local tissue blood flow in response to central hypovolemia is a major cause of reduced regional oxygen in this laboratory model. These observations are consistent with the work of Fadel et al. (11) who simultaneously measured relative changes in forearm oxygenated hemoglobin plus myoglobin, blood flow, and vascular conductance during LBNP between -10 and -50 mmHg. These authors showed strong correlations between NIRS changes and both blood flow and vascular conductance. Our work demonstrates that there is an inverse relationship between NIRS-determined tissue oxygenation and TPR from the earliest levels of hypovolemia to the point of presyncope.

It has been known for many years that one of the earliest compensatory mechanisms in hemorrhage is sympathetically mediated reflex vasoconstriction (1). During hemorrhage, vasoconstriction is heterogeneous throughout the body, predom-

Table 1. *Hemodynamic and metabolic parameters*

Parameter	Baseline Value	Statistically Significant Value	LBNP Level (mmHg) Where Statistically Different From Baseline
Arterial oxygen saturation, %	97.7±0.4	NA	none
Mean arterial pressure, mmHg	101.3±3.1	91.2±5.3	−90
Heart rate, beats/min	64.6±6.2	86.8±5.6	−60
Pulse pressure, mmHg	56.4±3.0	49.2±2.5	−45
Stroke volume, ml	140.2±7.4	129.8±7.9	−15
NIRS muscle SO₂, %	63.0±2.7	58.2±2.7	−15
NIRS muscle PO₂, mmHg	33.3±1.5	30.8±1.3	−15
NIRS muscle pH, pH units	7.44±0.01	7.41±0.01	−70

Values are means $\pm$ SE for baseline and lower body negative pressure (LBNP) level of siignificant change. NA, not applicable; NIRS, near infrared spectroscopy.
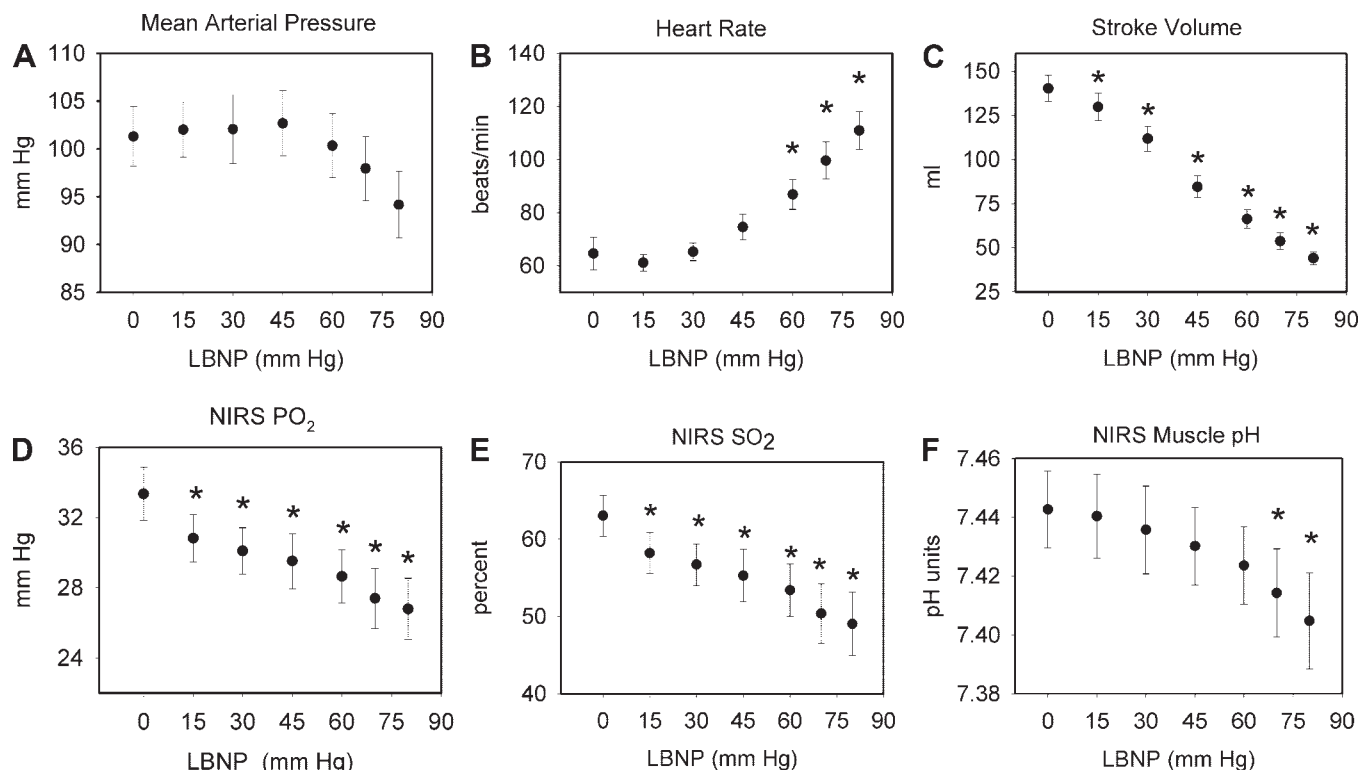
Fig. 1. Hemodynamic and near infrared spectroscopic (NIRS) derived parameters during lower body negative pressure (LBNP). Mean ± SE for all subjects ($n = 10$). Negative pressure is increased progressively from baseline (0). *$P < 0.05$ compared with baseline.

inantly affecting skeletal muscle and splanchnic circulations to redirect blood flow to the heart and brain (5, 13, 22). Our results complement a previous suggestion that progressive LBNP simulates the acute hemodynamic responses occurring during the early stages of hemorrhagic shock (9). One of the novel aspects of the current study is the demonstration that noninvasively determined skin and fat corrected SmO$_2$ can be used as an indication of this diversion of blood from the skeletal muscle (1), suggesting that it may be an early indication of hemorrhagic shock.

Figure 1 shows that pHm declined slowly until there was a large change in oxygen delivery, as evidenced by considerable reductions in SV and PmO$_2$. pHm is significantly decreased at an LBNP level of −70 mmHg, corresponding to a fall in PmO$_2$ to 27.4 ± 1.7 mmHg. We previously demonstrated a similar relationship between tissue pH and tissue PO$_2$ in swine liver

during hemorrhagic shock (27). In this animal study, measurements of tissue pH and PO$_2$ with invasive sensors demonstrated a breakpoint (PO$_2$crit) where pH began to decrease after tissue PO$_2$ had decreased to 22.3 ± 3.8 mmHg (linear model; Ref. 27), a value similar to that observed in this human study. These data provide evidence that LBNP causes a tissue metabolic disturbance (i.e., muscle dysoxia in the forearm) similar to that observed during actual bleeding.

PP has been suggested as an easy to obtain hemodynamic parameter that provides an early indication of the reduction in SV and oxygen delivery (6). In a study of 30 trauma patients requiring helicopter transport, PP was a better predictor of mortality than MAP, HR, or arterial oxygen saturation (8). The current study shows that noninvasive PmO$_2$ is an even earlier indicator of reduced oxygen delivery than PP (Table 1, Fig. 1). Likewise, transcutaneous oxygen tension (PtcO$_2$) has been
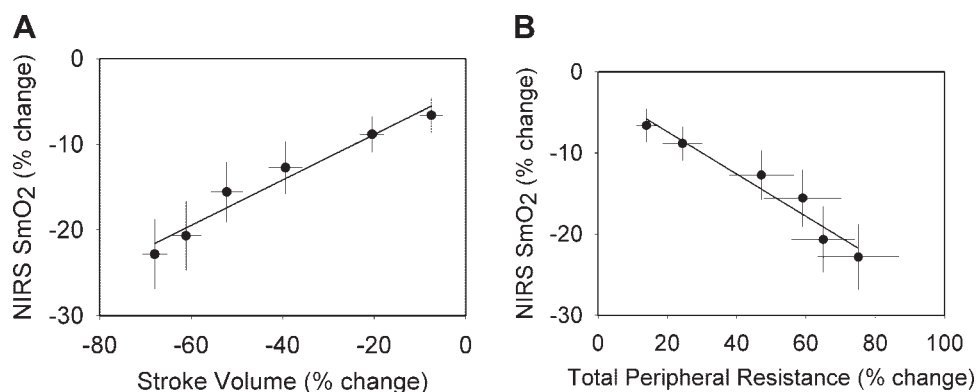

Fig. 2. Percent change from baseline for each level of LBNP. NIRS skin and fat corrected deep muscle oxygen saturation (SmO$_2$) is evaluated as a function of stroke volume, $r^2 = 0.96$ (A) and total peripheral resistance, $r^2 = 0.94$ (B). Error bars represent SE for all parameters.

assessed in emergency patients (31); nonsurvivors had significantly lower PtcO$_2$ values compared with survivors. However, application of PtcO$_2$ equipment to rapidly deteriorating patients is limited by the necessary 20 min equilibration time needed to heat the skin (31). Such a heating protocol is not necessary for NIRS technology, suggesting that it may be more appropriate for monitoring trauma patients. Indeed, the spectroscopic assessment of SmO$_2$ and PmO$_2$ is noninvasive, continuous, portable, and can be started rapidly in a trauma or emergency response. This monitoring technique has the potential to provide early warning of impending cardiovascular collapse in the pre- and early hospital settings.

Our laboratory model of progressive, central hypovolemia (LBNP) provides reproducible hemodynamic responses both within and between subjects; our hemodynamic results were similar to those obtained in previous studies in the same and other laboratories (7, 9, 23). While this model provides us with some insight into changes in tissue oxygenation during the initial phase of hemorrhagic shock, we cannot extrapolate our findings to monitoring of patients in septic shock. The microvascular response to sepsis is expected to have a different time course and oxygenation profile and is the subject of a separate patient study.

The NIRS techniques used in this study are unique in that they report values for PmO$_2$, SmO$_2$, and pHm deep within the muscle, corrected for light absorption by skin and fat. Other studies employing NIRS report only tissue oxygen saturation, where the measurement is a nonspecific weighted average of oxygen saturation in the skin, fat, and muscle depending on the design of the sensor (3, 10). Our sensor is specifically designed to collect and analyze spectra from the muscle, eliminating spectral interferences from skin pigment and fat (34). In addition, the calculation methods used to determine PmO$_2$ and SmO$_2$ are independent of variations in muscle optical properties between subjects. However, the pHm calculation methods rely on applying a correction factor to account for subject-to-subject variation in muscle optical properties (35). The robustness of this correction factor may limit the absolute accuracy of the pHm measurement for sick individuals. Current work is investigating the limitations of the pH calculation and in providing accurate pHm determinations in both healthy and sick individuals. The PmO$_2$ calculation described in the APPENDIX does not correct the hemoglobin dissociation curve for changes in pH, however, for in this study, pH changes are very small. Future work will enhance the PmO$_2$ assessment by incorporating this additional information.

Conclusions. We demonstrated a noninvasive technique for the determination of SmO$_2$, PmO$_2$, and pHm in a clinical laboratory model that simulates hemorrhage in humans. SmO$_2$ and PmO$_2$ were found to be early indicators of a reduction in oxygen delivery, most likely resulting from increased vasoconstriction to shunt blood from the skeletal muscle to the heart and brain. Muscle pH begins to decrease only when oxygen levels are significantly reduced, suggesting that the decrease in pHm may signal the onset of dysoxia in the muscle tissue. This noninvasive, continuous technique lends itself to monitoring critically ill patients at risk for hemodynamic instability.

APPENDIX

The method for determining muscle oxygen saturation (SmO$_2$) is reported in detail by Yang et al. (36), but is described briefly here. SmO$_2$ is defined by *Eq. 1*:

$$SmO_2 = \frac{C_{(HbO_2+MbO_2)}\langle L \rangle}{C_{(HbO_2+MbO_2)}\langle L \rangle + C_{(Hb+Mb)}\langle L \rangle} \quad (1)$$

$$= \frac{C_{(HbO_2+MbO_2)}}{C_{(HbO_2+MbO_2)} + C_{(Hb+Mb)}}$$

where L is the average photon pathlength through the tissue, $C_{HbO_2+MbO_2}$ is the oxygenated heme concentration, and C_{Hb+Mb} is the deoxygenated heme concentration, Hb represents hemoglobin and Mb myoglobin.

Attenuation of light by the subject's tissue, $A_{exp}(\lambda)$ at wavelength λ is defined in *Eq. 2*:

$$A_{exp}(\lambda) = \ln\left[\frac{I_{ref}(\lambda)}{I(\lambda)}\right] \quad (2)$$

where $I_{ref}(\lambda)$ is the measured diffuse reflectance intensity from a 99% diffuse reflectance reference standard at wavelength λ, $I(\lambda)$ is the measured diffuse reflectance intensity from the subject at wavelength λ. Incident light attenuation by tissue is caused by both absorption and scattering events. Light is absorbed by hemoglobin in the small blood vessels and myoglobin in the cells, as well as both intravascular and extravascular water and melanin pigment in the skin. Light is scattered away from physical structures in the tissue such as blood vessels and muscle fibers, as well as fat that lies over the muscle.

Muscle or tissue oxygen saturation can be calculated from measured spectra by assuming that light attenuation is primarily a result of absorption by oxygenated and deoxygenated hemoglobin and myoglobin, as well as a result of the scattering by the tissue. Several methods have been proposed for acquiring the spectra and performing the calculations; these methods are reviewed for application in physiology by Ferrari et al. (12). All of these methods involve fitting the measured attenuation spectrum to different mathematical models that described light penetration through the tissue to separate absorption from scattering and then fitting the obtained absorption spectra to the Beer-Lambert Law, which relates the absorption to the heme concentration. Primary differences between methods relate to how light scattering is measured and separated from the absorption. Light scattering can be measured directly with spatially resolved continuous
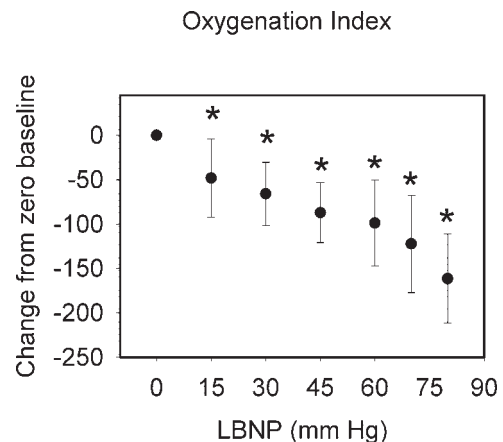

Fig. 3. Change from baseline oxygenation index (OI). OI at baseline is set to zero, changes measured in optical density (OD) units. Mean ± SE for all subjects ($n = 10$). Negative pressure is increased progressively from baseline (0). *$P < 0.05$ compared with baseline.

wave (CW) spectroscopy, time-resolved spectroscopy, and frequency-domain spectroscopic techniques. Recently van Beekvelt et al. (32) and Homma et al. (14) demonstrated that fat layers can influence the accuracy of an SmO$_2$ calculation. We demonstrated a method to correct attenuation spectra for the spectral interference of fat prior to their use in calculating physiologically important parameters (34).

To calculate SmO$_2$, we first remove the components of the spectrum that result from skin pigment absorption and fat scattering by using a two-source fiber optic probe. One source is placed close (2.5 mm) to the fiber optic bundle that transmits light to the spectrometer. This captures light from only the skin and fat layers. The second source, a farther distance from the detector bundle (30 mm), captures light from the skin, fat, and muscle layers. Light collected from the short distance pair is orthogonalized with the light from the long distance pair to generate a spectrum that describes attenuation from only the muscle layer. The details of this method are described in a prior publication (34). The corrected spectrum is then used for the calculation of SmO$_2$ based on an adaptation of a method first proposed by Stratonnikov and Loschenov (30). In this method, a Taylor expansion attenuation model is used to model light that penetrates through the tissue. The light absorption is modeled by Beer's law and that of the scattering is modeled as a Taylor expansion term.

The skin color and fat corrected attenuation spectrum is then described with the Taylor series expansion model A$_{model}$ detailed by Stratonnikov and Loschenov (30)

$$A_{model}(\lambda) = \ln\left(\frac{I_0(\lambda)}{I(\lambda)}\right) = (c_0 + c_1\lambda) + <L>\{c_{Hb+Mb}\,\varepsilon(\lambda) \\ + c_{HbO_2+MbO_2}\varepsilon_{HbO_2}(\lambda) + c_{wat}\varepsilon_{wat}(\lambda)\}\ln(10) \quad (3)$$

where I$_0$ is the light source intensity, c$_0$ and c$_1$ are constants, c$_{wat}$ is the concentration of water. ϵ_{Hb}, ϵ_{HbO_2}, and ϵ_{wat} are known extinction coefficients of Hb, HbO$_2$, and water, respectively. Since hemoglobin and myoglobin have nearly identical extinction coefficients, only the extinction coefficients of hemoglobin are required. The function (c$_0$ + c$_1\lambda$) describes the portion of the spectrum resulting from light that is scattered, as well as the wavelength-independent absorption caused by chromophores other than heme and water and the experimental difference caused by using I$_{ref}$ in *Eq. 2* as the incident light intensity (I$_0$) when calculating the attenuation spectra.

c$_0$, c$_1$ as well as c$_{Hb+Mb}$, c$_{HbO_2+MbO_2}$, c$_{wat}$, and *L* are obtained by nonlinear least square fitting of the measured attenuation spectrum A$_{exp}$ to the modeled spectrum A$_{model}$ described by *Eq. 3*. Once c$_{Hb+Mb}$ and c$_{HbO_2+MbO_2}$ are obtained, SmO$_2$ is calculated using *Eq. 1*. One of the limitations of this technique is the inability to separate the deoxygenation of myoglobin from hemoglobin, hence, the general name muscle oxygen saturation.

The partial pressure of oxygen in the muscle (PmO$_2$) can be calculated from SmO$_2$ determined with this method. Severinghaus (25) describes the relationship between SO$_2$ and PO$_2$ under standard physiological conditions:

$$PO_2 = \exp(0.385\cdot\ln(SO_2^{-1} - 1)^{-1} + 3.32 \\ - (72\cdot SO_2)^{-1} - (SO_2^6)/6) \quad (4)$$

For our application, SmO$_2$ is calculated from skin pigment and fat-corrected spectra. Then PmO$_2$ is calculated using *Eq. 4*. Again, PmO$_2$ represents an average of hemoglobin and myoglobin oxygen tension. We also recognize that calculation of PmO$_2$ should be compensated for variation in pH and PCO$_2$. Figure 1 shows that changes in pH were minimal in this LBNP model, with significant decreases in pH occurring late in the progression. For this reason, measurement of PmO$_2$ during early hypovolemia will be unaffected by this omission.

The calculations were implemented in software written in Matlab [version 7.0.4.365 (R14) Service Pack 2, Mathworks, Natick, MA]. The fitting algorithm was implemented with the "lsqcurvefit" function in the Matlab optimization toolbox version 3.0.2.

Comparison with alternate CW NIRS techniques. The new NIRS methodology is compared with a traditional analysis technique. Spectra from the long distance sensor, prior to correction for skin color and fat, were used with the UCL6 algorithm (19). This algorithm has been used on the NIRO-1000 instrument (Hamamatsu Photonics KK). The algorithm calculates relative values of oxyheme (ΔHbO$_2$) and deoxyheme (ΔHb) with six discrete values from the NIR spectrum. Delta represents the change from baseline absorbance at the six key wavelengths in optical density units. To compare to our calculated SmO$_2$, we then used the ΔHbO$_2$ and ΔHb values to determine the oxygenation index (OI) as described in Ferrari et al. (12).

$$OI = \Delta HbO_2 - \Delta Hb \quad (5)$$

OI, a measure of the relative changes in tissue oxygenation is illustrated in Fig. 3. This relative measure shows the same trends and statistical significance as the determination of PmO$_2$ (Fig. 1*D*) and SmO$_2$ (Fig. 1*E*). OI does not take into account subject variation in skin color, fat content, or muscle scattering, so only relative changes in tissue oxygenation during progressive LBNP can be assessed (19).

Our study uses LBNP to simulate progressive bleeding and seeks to identify a noninvasive spectroscopic parameter that can be used by first responders to determine if a patient is at risk for cardiovascular collapse. Since it will often be the case that the baseline condition will be unknown, relative measures of tissue oxygenation will be of limited value. The new NIRS algorithms presented here produce repeatable values for SmO$_2$ and PmO$_2$ across multiple subjects at varying levels of hypovolemia-induced vasoconstriction. These parameters have the potential to be useful in the treatment of critically ill patients; the next step is to validate the technique in actual patients.

DISCLOSURES

B. R. Soller is co-founder of Reflectance Medical with >5% interest. B. R. Soller, Y. Yang, and O. O. Soyemi are coinventors of the NIRS technology and could gain financially from its commercial development in agreement with the University of Massachusetts' policy of sharing its licensing income with inventors.

REFERENCES

1. **Barcroft H, Edholm OG, McMichael J, Sharpey-Schafer EP.** Post-haemorrhagic fainting: study by cardiac output and forearm flow. *Lancet* 15: 489–490, 1944.
2. **Becker LB, Weisfeldt ML, Weil MH, Budinger T, Carrico J, Kern K, Nichol G, Shechter I, Traystman R, Webb C, Wiedemann H, Wise R, Sopko G.** The PULSE initiative: scientific priorities and strategic planning for resuscitation research and life saving therapies. *Circulation* 105: 2562–2570, 2002.
3. **Beilman GJ, Groehler KE, Lazaron V, Ortner JP.** Near-infrared spectroscopy measurement of regional tissue oxyhemoglobin saturation during hemorrhagic shock. *Shock* 12: 196–200, 1999.

4. **Bellamy RF.** The causes of death in conventional land warfare: implications for combat casualty care research. *Military Med* 149: 55–62, 1984.

5. **Berne RM, Levy MN.** Interplay of central and peripheral factors in the control of circulation. In: *Cardiovascular Physiology.* St. Louis: Mosby, 1997, p. 269–285.

6. **Convertino VA, Cooke WH, Holcomb JB.** Arterial pulse pressure and its association with reduced stroke volume during progressive central hypovolemia. *J Trauma* 61: 629–634, 2006.

7. **Convertino VA, Ludwig DA, Cooke WH.** Stroke volume and sympathetic responses to lower-body negative pressure reveal new insight into circulatory shock in humans. *Auton Neurosci* 111: 127–134, 2004.

8. **Cooke WH, Convertino VA.** Heart rate variability and spontaneous baroreflex sequences: implications for autonomic monitoring during hemorrhage. *J Trauma* 58: 798–805, 2005.

9. **Cooke WH, Ryan KL, Convertino VA.** Lower body negative pressure as a model to study progression to acute hemorrhagic shock in humans. *J Appl Physiol* 96: 1249–1261, 2004.

10. **Crookes BA, Cohn SM, Bloch S, Amortegui J, Manning R, Li P, Proctor MS, Hallal A, Blackbourne LH, Benjamin R, Soffer D, Habib F, Schulman CI, Duncan R, Proctor KG.** Can near-infrared spectroscopy identify the severity of shock in trauma patients? *J Trauma* 58: 806–813, 2005.

11. **Fadel PJ, Keller DM, Watanabe H, Raven PB, Thomas GD.** Noninvasive assessment of sympathetic vasoconstriction in human and rodent skeletal muscle using near-infrared spectroscopy and Doppler ultrasound. *J Appl Physiol* 96: 1323–1330, 2004.

12. **Ferrari M, Mottola L, Quaresima V.** Principles, techniques, and limitations of near infrared spectroscopy. *Can J Appl Physiol* 29: 463–487, 2004.

13. **Gutierrez G, Reines HD, Wulf-Gutierrez ME.** Clinical review: hemorrhagic shock. *Crit Care* 8: 373–381, 2004.

14. **Homma S, Fukunaga T, Kagaya A.** Influence of adipose tissue thickness on near infrared spectroscopic signals in the measurement of human muscle. *J Biomed Opt* 1: 418–424, 1996.

15. **Imholz BP, Settels JJ, van der Meiracker AH, Wesseling KH, Wieling W.** Non-invasive continuous finger blood pressure measurement during orthostatic stress compared with intra-arterial pressure. *Cardiovasc Res* 24: 214–221, 1990.

16. **Imholz BP, van Montfrans GA, Settels JJ, van der Hoeven GM, Karemaker JM, Wieling W.** Continuous non-invasive blood pressure monitoring: reliability of Finapres device during the Valsalva manoeuvre. *Cardiovasc Res* 22: 390–397, 1988.

17. **Kubicek WG, Karnegis JN, Patterson RP, Witsoe DA, Mattson RH.** Development and evaluation of an impedance cardiac output system. *Aerospace Med* 37: 1208–1212, 1966.

18. **Majde JA.** Animal models for hemorrhage and resuscitation research. *J Trauma* 54: S100–S105, 2003.

19. **Matcher SJ, Elwell CE, Cooper CE, Cope M, Delpy DT.** Performance comparison of several published tissue near-infrared spectroscopy algorithms. *Anal Biochem* 227: 54–68, 1995.

20. **Newman DG, Callister R.** The non-invasive assessment of stroke volume and cardiac output by impedance cardiography: A review. *Aviat Space Environ Med* 70: 780–789, 1999.

21. **Parati G, Casadei R, Groppelli A, Di Rienzo M, Mancia G.** Comparison of finger and intra-arterial blood pressure monitoring at rest and during laboratory testing. *Hypertension* 13: 647–655, 1989.

22. **Peitzman AB, Billiar TR, Harbrecht BG, Kelly E, Udekwu AO, Simmons RL.** Hemorrhagic Shock. *Curr Probl Surg* 32: 927–1002, 1995.

23. **Sageman WS.** Reliability and precision of a new thoracic electrical bioimpedance monitor in a lower body negative pressure model. *Crit Care Med* 27: 1986–1990, 1999.

24. **Sauaia A, Moore FA, Moore EE, Moser KS, Brennan R, Read RA, Pons PT.** Epidemiology of trauma deaths: a reassessment. *J Trauma* 38: 185–193, 1995.

25. **Severinghaus JW.** Simple, accurate equations for human blood O$_2$ dissociation computations. *J Appl Physiol* 46: 599–602, 1979.

26. **Soller BR, Cingo NA, Puyana JC, Khan T, Hsi C, Kim H, Favreau J, Heard SO.** Simultaneous measurement of hepatic tissue pH, venous oxygen saturation and hemoglobin by near infrared spectroscopy. *Shock* 15: 106–111, 2001.

27. **Soller BR, Heard SO, Cingo N, Hsi C, Favreau J, Khan T, Ross RR, Puyana JC.** Application of fiberoptic sensors for the study of hepatic dysoxia in swine hemorrhagic shock. *Crit Care Med* 29: 1438–1444, 2001.

28. **Soller BR, Idwasi PO, Balaguer J, Levin S, Simsir SA, Vander Salm TJ, Collette H, Heard SO.** Noninvasive, NIRS-measured muscle pH and PO$_2$ indicate tissue perfusion for cardiac surgical patients on cardiopulmonary bypass. *Crit Care Med* 31: 2324–2331, 2003.

29. **Soyemi O, Landry M, Yang Y, Soller BR.** Standardization method for correcting spectral differences across multiple units of a portable near infrared-based medical monitor. *Proc SPIE* 5702: 135–142, 2005.

30. **Stratonnikov AA, Loschenov VB.** Evaluation of blood oxygen saturation in vivo from diffuse reflectance spectra. *J Biomed Opt* 6: 457–467, 2001.

31. **Tatevossian RG, Wo CC, Velmahos G, Demetriades D, Shoemaker WC.** Transcutaneous oxygen and CO2 as early warning of tissue hypoxia and hemodynamic shock in critically ill emergency patients. *Crit Care Med* 27: 2248–2253, 2000.

32. **Van Beekvelt MC, Borghuis MS, van Engelen BG, Wevers RA, Colier WN.** Adipose tissue thickness affects in vivo quantitative near-IR spectroscopy in human skeletal muscle. *Clin Sci* 101: 21–28, 2001.

33. **Wesseling KH, Settels JJ, van der Hoeven GM, Nijboer JA, Butijn MW, Dorlas JC.** Effects of peripheral vasoconstriction on the measurement of blood pressure in a finger. *Cardiovasc Res* 19: 139–145, 1985.

34. **Yang Y, Landry MR, Soyemi OO, Shear MA, Soller BR.** Simultaneous correction of skin color and fat thickness for tissue spectroscopy using a two-distance fiber optic probe and orthogonalization technique. *Opt Lett* 30: 2269–2271, 2005.

35. **Yang Y, Shoer L, Soyemi OO, Landry MR, Soller BR.** Removal of analyte-irrelevant variation in near infrared tissue spectra. *Appl Spectrosc* 60: 1070–1077, 2006.

36. **Yang Y, Soyemi OO, Scott PJ, Landry MR, Lee SMC, Stroud L, Soller BR.** Quantitative measurement of muscle oxygen saturation without influence from skin and fat using continuous-wave near infrared spectroscopy. *Opt Exp* 15: 13715–13730, 2007.

37. **Zhang S, Soller BR, Micheels RH.** Partial least-squares modeling of near-infrared reflectance data for noninvasive in vivo determination of deep-tissue pH. *Appl Spectrosc* 52: 400–406, 1998.